Characterization of XeF_2 Etching for Release of Piezoelectric Micro-Robots

Ramon Alonso

Mechanical Engineering, San Joaquin Delta College

NNIN REU Site: Lurie Nanofabrication Facility, University of Michigan, Ann Arbor, MI
NNIN REU Principal Investigator: Prof. Kenn Oldham, Mechanical Engineering, University of Michigan, Ann Arbor
NNIN REU Mentor: Jongsoo Choi, Mechanical Engineering, University of Michigan, Ann Arbor
Contact: ralonso766@students.deltacollege.edu, oldham@umich.edu, jongs@umich.edu

Abstract and Introduction:

Thin-film piezoelectric micro-robots could potentially help save human lives with their ability to do reconnaissance in hazardous places, or help avoid costly demolition processes during infrastructure maintenance by utilizing images provided from inconvenient and/or unreachable locations. In order to achieve these goals, there should be an optimized fabrication process for these micro-robots using microelectromechanical systems (MEMS) technology.

A critical fabrication step in MEMS technology is the safe release of these micro-robots using xenon difluoride (XeF_2) etching, which etches only silicon in an isotropic manner. Due to the nature of isotropic etching, the etching results depend on the amount and location of the silicon's open surface area. Micro-robots can also be designed with trenches such that XeF_2 gas flows through the trenches and undercuts piezoelectric actuators, allowing free movement. Thus, the geometry and location of the trenches is important to successfully release micro-robots.

In this work, XeF_2 etching of several piezoelectric micro-robot designs have been characterized, which can be used to modify the design of the micro-robots for a faster and safer release. Additionally, the etching of C_4F_8 polymer, which was deposited on the side wall of the trenches in deep reactive ion etching (DRIE), was characterized after the polymer was observed to protect silicon from being etched.

Experimental Procedure:

Characterization of Fluorocarbon Polymer. Polymer etching was tested using modules containing dummy micro-robotic devices fabricated from silicon oxide and gold. Images were taken of each module using the scanning electron microscope (SEM). Then, tape was placed on the module to prevent the fluorocarbon polymer from being deposited at certain locations. Next, a fluorocarbon polymer was deposited on the module. Afterword, the tape was removed confirming the polymers presence. Subsequently images were taken using the SEM to further verify the presence of the fluorocarbon polymer. The SEM also provided the thickness of the polymer where the tap was. Later the fluorocarbon polymer was removed using an oxygen based recipe. This recipe was then confirmed to remove the fluorocarbon polymer after SEM images showed no fluorocarbon polymer on the module.

Releasing Micro-Robotic Devices. XeF_2 etching was completed on silicon wafer modules containing between one and fifteen micro-robotic devices of various shapes. First, the module was mounted with the backside exposed on a six-inch silicon wafer with crystal bond. Then the sample was etched with reactive ion etching (RIE), removing the oxide layer. Next the module was etched using deep reactive ion etching (DRIE) process to etch away the silicon until there was visible etching on the module. Subsequently the module was removed from the silicon wafer and the photoresist (PR) material was removed from the module. The cleaned module was mounted with the topside exposed on a silicon wafer and then placed in the STS Pegasus to remove the residual Teflon® using the oxygen-based cleaning recipe. Later, the module was detached from the silicon wafer and cleaned. Thereafter the module was mounted with the backside exposed on a silicon wafer and the DRIE process was continued until the oxide layer was visible.

The wafer was then placed in hot water until the module released from the wafer. To prepare for XeF_2 etching, the module was placed on a glass slide and taped along the edges to prevent XeF_2 from etching the sidewalls of the module. The module was etched with XeF_2 until the sample was released from the wafer as it was designed to do. Finally the top side's protective oxide layer was removed from the module.

Results:

Two patterns were observed after completing the XeF_2 etching process on the modules. The first pattern was that micro-robotic devices designed with the same geometry would have similar etch rates and releasing times. This pattern emerged regardless of where the micro-robotic devices were located on the module. Some samples observed were located as far as 1000 microns from each other.

The second pattern demonstrated how the amount of time needed to release the micro-robotic devices was heavily dependent upon the geometry of the backside etching area. It was found that a greater etching area on the backside led to a significantly faster release of the micro-robot.

Conclusion and Future Works:

Through the releasing of different micro-robots, we were able to determine that the etch rate is dependent upon the number of micro-robotic devices on a module and the geometry of those devices. However, the most significant factor is the geometry of the backside etching area. Therefore, if a module has devices with different geometry and/or backside etching areas, they will be released at different times. This results in over-etching of the faster-releasing devices, making them unusable. Accordingly, we suggested alterations for the area of the backside etching on devices that have more geometric features, in order to reduce the etching time and release all of the micro-robotic devices at the same time. With these changes in place it would be possible to increase the yield of adequately released micro-robots.

In the future, the group would be able to test this theory with more fabricated micro-robotic devices using these design changes. Also the group would be able to characterize the micro-robotic devices to find the optimum design and integrate them in the final micro-robot.

Acknowledgments:

I would like to thank Professor Oldham for supporting me through this intensive internship. I would also like to thank Jongsoo Choi for training me and helping me through all the roadblocks that this research presented. I would finally like to thank the NNIN REU Program, NSF and LNF lab for providing funding and the opportunity to experience this wonderful internship.

Two-Dimensional Buckled Nanoscale Nanomembrane as Tunable Grating

Adel Azghadi

Mechanical Engineering, Los Angeles Pierce College

NNIN REU Site: ASU NanoFab, Arizona State University, Tempe, AZ

NNIN REU Principal Investigator: Dr. Hanqing Jiang, Associate Professor of Mechanical Engineering, School for Engineering of Matter, Transport and Energy, Arizona State University

NNIN REU Mentor: Teng Ma, Research Associate in Mechanical Engineering, School for Engineering of Matter, Transport and Energy, Arizona State University

Contact: adelazghadi@aol.com, hanqing.jiang@asu.edu, tengma@asu.edu

Abstract:

We have developed a tunable, optical two dimensional (2D) grating which can be used for measuring thermal-induced strain based on buckled thin film with periodic sinusoidal patterns on elastomeric substrates. One dimensional (1D) sinusoidal gratings and 2D herringbone gratings with a submicron scale have been fabricated with nanometer-thick gold (Au) film coated on uniaxial and biaxial pre-tensioned polydimethylsiloxane (PDMS) substrates, respectively. Due to the competition between the soft elastomeric substrates and relatively stiff Au films, uniform periodic wavy profiles are created upon releasing the pre-tension. The level of pre-strain, the mechanical properties of the PDMS and Au, and the thicknesses of Au films determine the amplitudes and wavelengths of wavy structures. The buckling profiles can be tuned mechanically by changing the level of pre-strain applied on the elastomeric substrate. Moreover, characteristics of the buckles vary based on the thickness of the stiff Au nanomembrane. Different methods of producing a stiff film on top of an elastomeric substrate have been established so far, while for this project, we focused on deposition of Au on PDMS by plasma sputter coating to create 2D herringbone buckles, which has the advantage of being low cost and extremely time efficient.

Introduction:

During the past few years the reliability of electronics packaging has received increasing attention, due to the soaring sales of iPhone and iPad. There are various electronic packaging failure modes like cracking, delamination and fatigue. Among them, the most well-known and often investigated mechanics issue for electronic packages is interface reliability. There is a great need for characterizing the deformations and strains in interfaces to the thermo-mechanical loadings caused by coefficient of thermal expansion (CTE) mismatches. Strain sensor using optical grating is a relatively new experimental mechanics method for measuring deformation and strain. Our method of making a buckled thin film on PDMS as a grating provides the capability of making uniform patterns at micro and submicron lever spontaneously without conventional photolithography techniques. More importantly, the wavelengths of buckling structure can be easily controlled by the thickness of Au film deposition at nanometer level which enables great tunability for optical grating.

Experimental Procedure:

The first part of our project was producing 1D ripples in Au nanomembrane stiff films. First, a thin slide of polydimethylsiloxane (PDMS) was prepared by mixing silicone elastomeric base and curing agent at the ratio of 10:1 by weight. After curing the PDMS at 80°C for three hours, we applied a desirable pre-strain on our substrate by mechanical stretcher only in one direction (x-direction). A thin layer of Au was coated on top of the pre-tensioned substrate by argon plasma-assisted sputter coating. Finally, releasing the pre-strain in the PDMS led to a compressive force in the Au film as the PDMS relaxed to zero strain, leading to periodic buckling.

In the second part of our research, we focused on 2D herringbone nanomembrane buckling. 2D samples were prepared with almost the same procedure as 1D, except that in the second step, we stretched our substrates in both X and Y directions sequentially (first in X and then in Y direction). Also, after coating the pre-stretched substrate with Au, the sample had to be released sequentially in both directions, but in reverse order (first in Y, then in X direction). This time, by releasing the sample 2D zigzag shape, buckling appeared in the nanomembrane.

Results:

Four 1D sample wavelengths and amplitudes of nanomembrane ripples were studied throughout the project. Figure 1 shows us the possible relationships [1] for amplitude and wavelength of the buckles based on thickness of the Au layer and level of pre-strain. The buckling period, amplitude, pre-strain and thickness of the Au film are characterized by "λ", "A", "ε_{pre}" and "h_f" respectively. Coating time determined the thickness of the Au nanomembrane linearly, and every thirty seconds corresponded to 5 nm.

Based on graphs in Figure 2, by increasing the coating times, both wavelength and amplitude of buckles became larger.

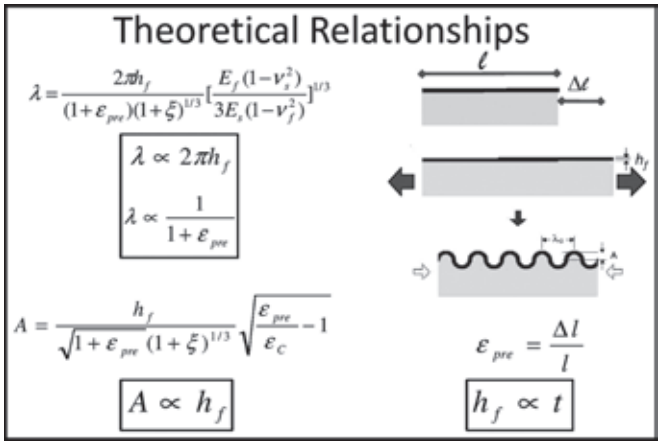

Figure 1: Theoretical relationships.

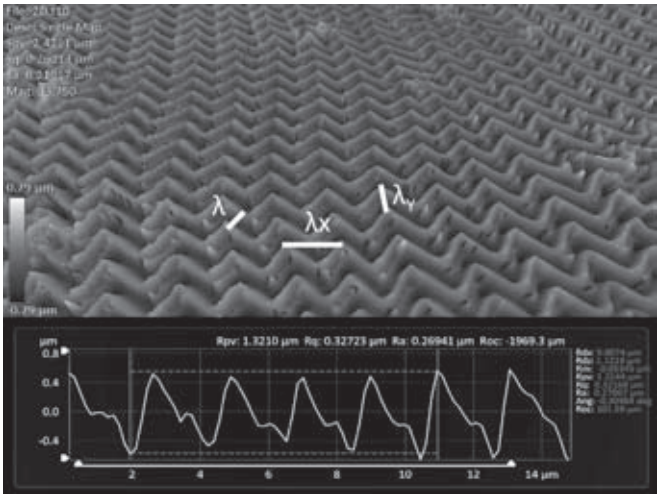

Figure 3: Optical profilometer image, 2D buckling, deposition time is 2.5 min, pre-strain of 15%.

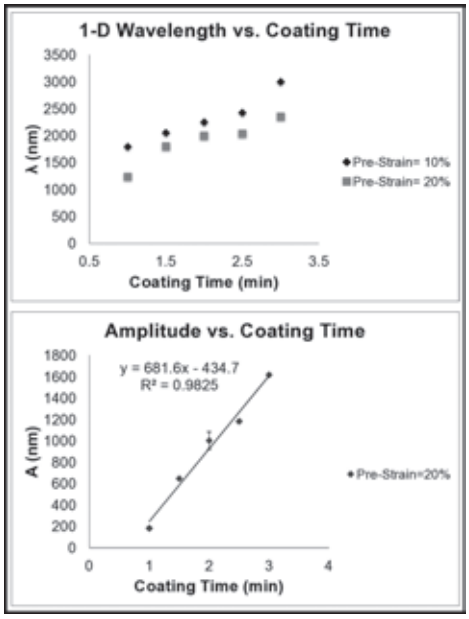

Figure 2: a) 1D wavelength vs. coating time graph, b) amplitude vs. coating time graph.

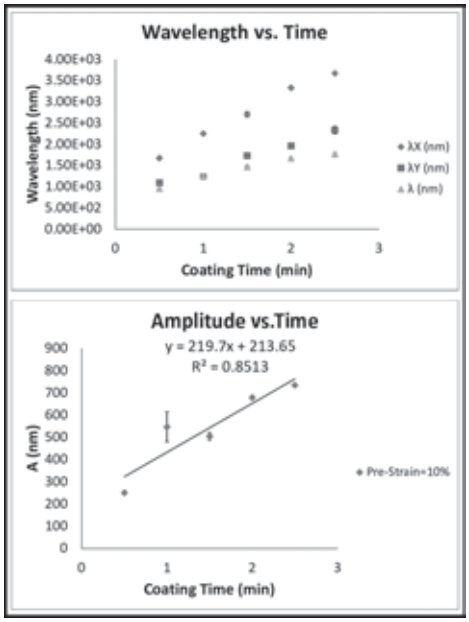

Figure 4, left: 2D wavelengths vs. coating time graph, b) amplitude vs. coating time graph.

Also as pre-strain became larger the wavelength of the ripples decreased. These results supported our theoretical relationships.

Figure 3 is the 3D image of 2D buckles using optical profilometer. For each 2D buckle, three different wavelengths were measured, λ_x, λ_y and λ, in X, Y and normal to buckle direction, respectively. Figure 4 shows that all three types of wavelengths are in direct relationship to the coating time. Also amplitude of the wrinkling profile increases when coating time increases. These results also are a proof to our theoretical relationships.

Future Work:

In 2D buckles by increasing the pre-strain to even a greater level (25%-50%), the smallest wavelength (λ) was inversely proportional to the pre-strain, which means that as we stretched our samples to a greater extend, the wavelength of the buckles became smaller. Also if we can find a way to coat a thinner layer of gold, we might be able to produce gratings with wavelength closer to the wavelength of the natural light by even a smaller pre-strain. Moreover, we found out that creating a 2D herringbone structure in relatively stiff nanomembrane gold film on top of PDMS by argon plasma sputter coating is a low cost and time-efficient method.

Acknowledgements:

At this point I would like to thank my principal investigator Dr. Hanqing Jiang and my mentor Teng Ma for the time that they have spent with me this summer and all they have taught me. Also I would like to say thank you to Dr. Trevor Thornton, our site coordinator at Arizona State University, and the Center for Solid State Electronic Research (CSSER). Finally I would like to thank the NNIN REU Program and the National Science Foundation for funding this program.

References:

[1] Cunjiang, Y; "Forming wrinkled stiff films on polymeric substrates at room temperature for stretchable interconnects applications"; Thin Solid Films, 519, 819 (2010).

Nanoparticle Sorting in Microfluidic Channels

Rachel Baarda
Physics, University of Utah

NNIN REU Site: Nanotech, University of California, Santa Barbara, CA
NNIN REU Principal Investigator: Professor Andrew Cleland, Physics, University of California, Santa Barbara
NNIN REU Mentor: Dr. Sukumar Rajauria, Physics, University of California, Santa Barbara
Contact: rabaarda@gmail.com, anc@physics.ucsb.edu, sukumar.rajauria@gmail.com

Abstract:

A device capable of detecting, characterizing and sorting nanoparticles and important biological targets would be an invaluable tool both for public health monitoring and for biomedical research. We describe the development of a microfluidic device that should permit the high-throughput sorting of nanoparticles, potentially able to sort hundreds to thousands of particles per second.

Introduction:

The ability to manipulate biologically relevant nanoparticles such as viruses, proteins, and synthetic nanoparticles would be a boon for medical research. Examples of the utility of such a device include aggregating rare particle types or efficiently imaging representative particles in a diverse mixture. Current methods of sorting particles are impractical for use in processing polydisperse samples. We describe the development of a microfluidic device that should permit high-throughput nanoparticle sorting. The device consists of a microchannel, an optical sensor, and a fluid actuator. Sorting is accomplished by driving fluid on-demand using a piezoelectric transducer (PT), actuated by an optical sensor sensitive to particles passing through the microchannels. We have performed a systematic study of PT actuation using a laser vibrometer, and have explored various means of coupling the PT and the microfluidic device. Through this study, we have developed an improved method for mounting the PTs to the microfluidic device that we expect will demonstrate more effective fluid actuation.

Experimental Procedure:

Device Fabrication. The device's microchannels were cast in the transparent elastic polymer polydimethylsiloxane (PDMS). The mold used to cast the PDMS consists of patterned SU-8 photoresist. PDMS was spun onto the mold, then cured on a hotplate for 10-15 minutes at 140°C. We coupled the PTs to the microchannels by embedding them in a second layer of PDMS, which was cured for 20-40 minutes at 140°C. Each of the two PTs was placed over a reservoir which directed fluid perpendicular to the direction of particle flow (see Figure 1). Once the PDMS had hardened, we peeled it from the mold and cored ports for fluid injection using a biopsy punch. We prepared the PDMS for bonding by exposing it to UV ozone, and then we bonded it to a glass substrate and cured it for 3-5 hours at 140°C. Fluid and florescent polystyrene nanoparticles were injected into the microchannels from pressurized reservoirs connected to flexible tubing inserted into the ports. Both PTs were connected to a function generator. Particles were forced through a fluid restriction and detected by an optical sensor, which signaled the function generator to actuate the PTs to direct the particle as desired.

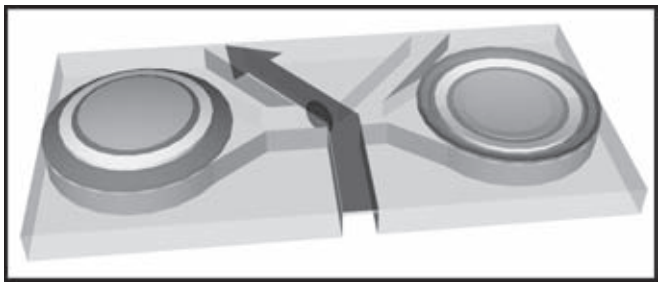

Figure 1: Particle actuation.

Device Characterization. Piezoelectric materials deform mechanically in response to applied voltage. We induced sinusoidal vibration in the PTs using a function generator with frequencies in the kilohertz range. We characterized these PTs and the PDMS that formed our device's channels using a laser vibrometer. This tool measures the vibration of a reflective surface by measuring the phase shift difference between the reflected laser beam and a reference beam.

Results and Conclusions:

We performed a variety of vibrometry experiments to determine the behavior of the device as driving voltage, frequency, and measurement location were varied.

We measured the resonance characteristics of the PTs by applying a fixed voltage to the PTs while modulating the driving frequency from 1-50 kHz. At each frequency, we found the peak-to-peak displacement of the PT as measured by the vibrometer. The resulting curve showed that the PTs act as harmonic oscillators with resonance frequencies close to 7 kHz, in accordance with the manufacturer's specifications. We performed these experiments on several PTs in three distinct environments: 1. The PT was glued onto a hollow metal cylinder. This showed the clearest resonant peak and two harmonics; 2. The PT was embedded in PDMS; and 3. The PT was embedded in PDMS and bonded to glass. In addition, the microchannels were filled with DI water. The results are summarized in Figure 2.

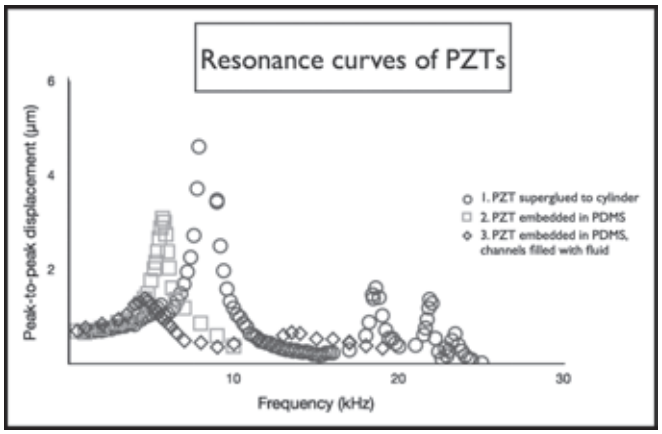

Figure 2: Resonance curves of PTs.

Because PDMS is an elastomer, we examined the possibility of vibrations propagating through it. We tested this by determining that the PTs were coupled together by PDMS vibrations: that is, we found that each PT could drive the respective other. When one PT was driven by the function generator, we found that the other PT showed a resonance curve similar to (though smaller than) that of the driving PT.

We examined the PDMS vibration further by measuring the PDMS itself. We applied a layer of silver paint to a sample to make it reflective and measured the peak-to- peak displacement of the PDMS as we moved the vibrometer beam away from the edge of the driving PT. The results, summarized in Figure 3, showed a standing wave in the PDMS whose amplitude was reduced when the sample was made of stiffer PDMS.

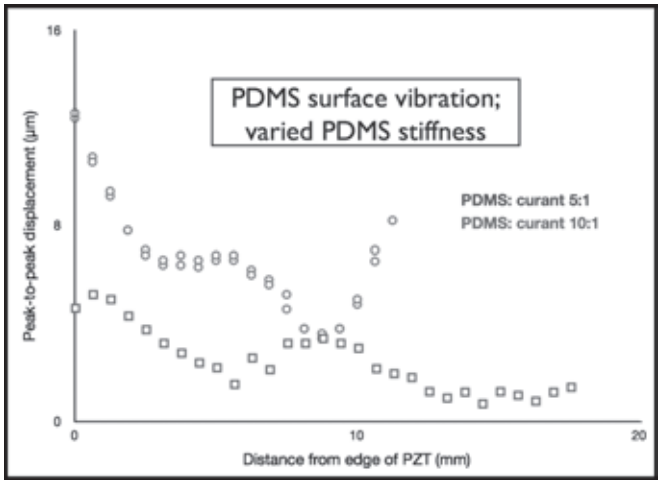

Figure 3: Standing waves in PDMS.

In light of these data, we desired a way to isolate the PT vibration from the PDMS so that fluid actuation would be discrete and well-controlled. This was accomplished by machining brass funnels on which the PTs could be mounted, the stems of which could be inserted into ports in the PDMS. Vibrometry measurements showed that this modification successfully isolated the PT vibrations from the PDMS: we repeated both experiments testing for PDMS vibration without finding a signal in any case.

Future Work:

Future direction for this project includes further calibrating the device to allow for well-controlled particle actuation. Once the device works predictably with the polystyrene nanoparticles, biological samples could begin to be processed.

Acknowledgments:

I would like to thank Sukumar Rajauria and Andrew Cleland for their exceptional guidance, Jorge Carvalho for his expertise in chemistry and Matlab, and Samantha Cruz for her advice and resourcefulness as program coordinator. I would like to acknowledge Chris Axline for beginning and developing this project. Finally, I would like to acknowledge and thank the National Nanotechnology Infrastructure Network Research Experience for Undergraduates Program and the National Science Foundation for funding this project.

Carbon Nanotube Microfluidic Channels for Cell Manipulation

Michael Bellavia
Bioengineering, SUNY Binghamton

NNIN REU Site: Lurie Nanofabrication Facility, University of Michigan, Ann Arbor, MI
NNIN REU Principal Investigator: Anastasios John Hart, Mechanical Engineering, University of Michigan, Ann Arbor
NNIN REU Mentor: Kendall Teichert, Mechanical Engineering, University of Michigan, Ann Arbor
Contact: mbellav1@binghamton.edu, ajohnh@umich.edu, kbt@umich.edu

Abstract and Introduction:

Due to their remarkable porosity (~99%), electrical and mechanical robustness, and ability to be chemically functionalized, vertically aligned carbon nanotubes ("CNT forests") are a promising material for use in lab-on-a-chip devices. Utilizing these in bio-MEMS (e.g. for bioparticle detection) provides several prospective advantages over conventional solid materials (polydimethylsiloxane or PDMS, silicon or Si). These include the capability for flow both around and through the nanoporous structures to increase particle-surface interaction and greater selectivity for small (e.g. 10 nm) particles [1].

Current literature has illustrated the prospects of CNT structures placed within the fluid flow. Alternatively, this project aimed to demonstrate the capability of CNT forests as microfluidic channel walls. Ultimately, flow through various geometries could be exploited for potential biomedical applications.

Via photolithography, patterns for flow channels were transferred onto a Si wafer. A base layer of alumina was deposited, overlaid with a layer of iron catalyst. The wafer was diced into individual devices then placed in a tube furnace and forest growth achieved by thermal chemical vapor deposition (CVD) using a mixture of helium, hydrogen, and ethylene, at 775°C.

Testing was accomplished with a benchtop fluidic system consisting of a syringe pump, acrylic/PDMS chip dock, and a camera-equipped stereoscope for visualization. Flow through the CNT channels was verified, and experiments using polystyrene beads and human monocytes suspended in the fluid flow were observed.

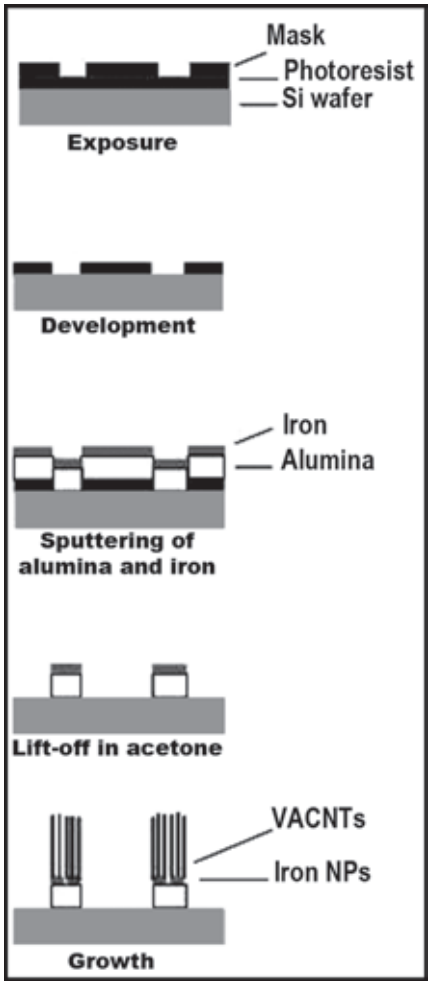

Figure 1: Step by step fabrication of microfluidic devices.

Methods:

Photolithography and sputtering (10 nm alumina and 1 nm iron) were implemented to define the catalyst regions for forest growth on a Si wafer. Afterwards, the wafer was diced into individual devices. CNT growth was performed in a tube furnace.

First the substrate was annealed in 100 sccm H_2 and 400 sccm helium (He) at 775°C for 10 minutes. Next, the substrate was removed from the furnace and allowed to cool in stagnant annealing gases (He, H_2). It was then re-inserted for growth in 400 sccm He, 100 sccm H_2, and 100 sccm C_2H_4 at 775°C for various durations. (See Figure 1.)

Difficulties in fluid transfer motivated particular mount designs. The initial concept was a short (≈ 1 cm) PDMS cylinder with a cavity extending upwards from the bottom to house the chip and forest. Holes were punched above the chip reservoirs and aligned to another punched from the side. A dispensing needle was placed in the side hole and connected via silicone tubing to a syringe pump. Fabricating the cavity properly proved challenging.

Once the PDMS covers contacted the forest, further adjustment would damage the forest. Further, leakage over the forest was noted. To circumvent this, an acrylic/PDMS chip docking system was developed (Figure 2a) and placed under a stereoscope. An adjustable stage, its vertical movement controlled by a micrometer, was positioned below an acrylic piece machined with vertical channels. These channels were aligned with the reservoirs of a bare silicon chip. A layer of PDMS with holes aligned to both those of the chip and the acrylic was placed on top of the chip. The stage was moved upward with the micrometer until the PDMS on the chip applied sealing pressure to the acrylic

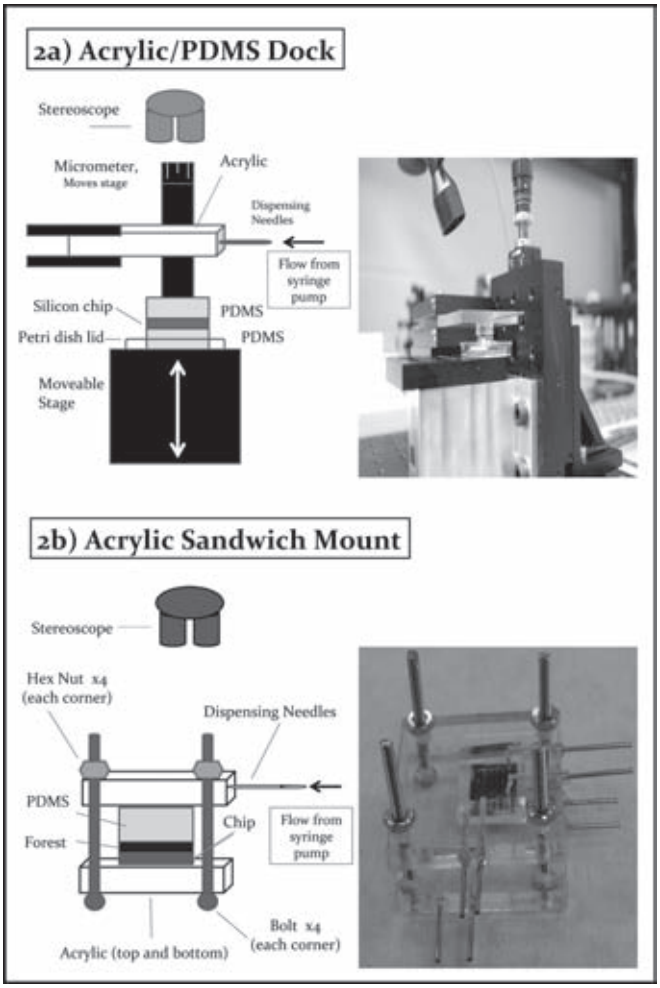

Figure 2: Schematics.

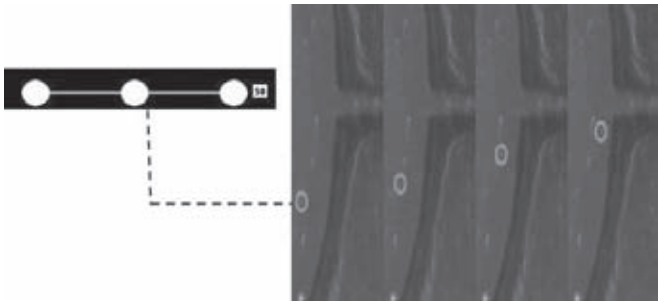

Figure 3: A monocyte (within the circle) moves from a reservoir into a channel. The frames (labeled 1-4) are each separated by a fourth of a second.

plate. An assortment of materials with different elasticity, such as rubber, foam, and PDMS were used as backing for the chip as a means of improving sealing to the acrylic. Flow tests were conducted at infusion rates between 30 μL/hr and 10 μL/min using 3, 10, and 15 μm polystyrene beads. Sandwiching the chip between $\approx$ 5 mm layers of PDMS was found to be adequate, as it most reliably prevented leakage.

A portable mount (Figure 2b) was constructed; a PDMS layer between two acrylic squares machined with vertical channels spaced to fit whatever device. With this, several flows of monocytes, a variety of white blood cell, were undertaken (Figure 3).

To simulate the pressure drops to be experienced in the flow, flow through certain designs was analyzed with COMSOL Multiphysics, a finite element software package. Pressures and velocities from select geometry were compared to pressure results found from a flow equation assuming rectangular channels cited in the Microfluidics and Nanofluidics Handbook by Mitra and Chakrabourty [1]. These flows will be related to experimental results in future work.

Results:

Preliminary flows of polystyrene beads and monocytes through CNT forests were performed successfully. Monocytes flowed rapidly even after the pump was stopped, but after a time, backflow occurred. This may be due to inadequate sealing. Imaging with the stereoscope camera did not provide satisfactory resolution. Further analyses might be conducted with fluorescence microscopy.

Close agreement was evident between the average velocities at the inlets for the COMSOL™ model and those of the fluidics equation. This asserts that COMSOL can be sensibly extrapolated to modeling other devices or new geometries.

Future Work:

The fluidic delivery system shall be improved and testing systematized for the procedure to be efficient and easily repeatable. The forests are fragile, necessitating more precise alignment strategies for the PDMS overlay such that sealing is obtained with less risk of harm to the forest. This would greatly expedite testing. A redesign of the flow geometries could contribute to this, and will be undertaken.

Optimization of the CNT growth conditions is required to fabricate CNT devices with consistent and repeatable fluidic properties. Further, the wealth of properties innate in CNTs such as photoluminescence as well as outstanding tensile strength and electrical conductance, make them attractive candidates for further integration in innovative microfluidic devices.

Acknowledgements:

I'd like to express my earnest gratitude for the guidance of Kendall Teichert. I am indebted to Professor John Hart and the Mechanosynthesis Group. Lastly, I'd like to thank the National Science Foundation and NNIN REU Program for this opportunity.

References:

[1] Fachin, F., et al., Journal of MEM Systems (2011): 1428-1438.

Fabrication of MEMS Using Cheap Substrates

Ryan Gaudreau
Engineering Science, Stony Brook University

NNIN REU Site: Howard Nanoscale Science and Engineering Facility, Howard University, Washington, DC
NNIN REU Principal Investigator: Dr. Gary L. Harris, Electrical Engineering, Howard University
NNIN REU Mentor: Dr. William L. Rose, Electrical Engineering, Howard University
Contact: ryan.gaudreau@yahoo.com, gharries@msrce.howard.edu, wbullrose@gmail.com

Abstract:

The objective of this project was to create microelectromechanical systems (MEMS) using paper as the substrate and piezoresistive carbon ink to create a device that was sensitive to force. The idea behind this approach was to minimize cost and maximize ease of production. To achieve our objective, we used a paper cantilever design to correlate the relationship between force and change in resistance of the device, and subsequently the relationship between current and applied force. Our results showed a linear relationship. The next part of the project required us to apply this relationship to create a useful device. We opted on creating a microphone made from paper and the piezoresistive material. This was based on the fact that the relationship between force and resistance would facilitate the modulation of current in much the same way as the moving coil in a magnetic field in a conventional microphone. We were able to successfully accomplish our goals after several designs were tested and optimized.

Introduction:

Microelectromechanical systems (MEMS) are becoming increasingly popular. MEMS are used today in many fields, from biotechnology, medicine, communications, to inertial sensing [1]. In an attempt to decrease cost and time of production, paper-based MEMS are now being researched as a cheap alternative [2]. A paper MEMS device does not require a clean room, takes less than an hour to make, and cost only cents to produce. These attributes make them very attractive.

Our project sought to use a piezoresistive material on a paper substrate in order to create a practical device. Our project was divided into two parts. The first part sought to examine the relationship between force and change of resistance/current on the piezoresistive material, and then in the second part, apply this in a practical way. We decided we could use the properties of the device to build a paper microphone.

Fabrication and Experimental Procedure:

The first part of our experimental procedure required us to design paper MEMS to test and correlate the relationship between force and resistance of the piezoresistive material. To do this we used the drawing software Corel Draw X5 to design cantilever systems. We then used an Epilog Helix Laser to cut the devices out. Carbon-based piezoresistive paint was applied to the device and allowed to dry, followed by a silver based conductive paint. A Wheatstone bridge was constructed on a breadboard to precisely measure the resistance of our device.

The MEMS was fixed onto a mounting device that slowly lowered the cantilever of the MEMS onto a precision balance, applying a measurable force. Applying force to the cantilever put force on the piezoresistor, therefore changing its resistance and causing current to flow through the ammeter. The adjustable resistor was then manipulated until the current read zero. The resistance of the adjustable resistor could then be read using a multi meter. Using the equation for a Wheatstone bridge, the resistance for the MEMS could be found and thus correlated to force.

We tested several single cantilevers and double cantilever designs applying the force and varied distance from the piezoresistive material (Figure 1). We were thus able to establish a relationship between the force and resistance, and consequently, current.

For the second phase of our procedure, we used the same fabrication process as above to design and cut out our piezoresistive paper microphone. We tested several designs to first create a working microphone and then to optimize it. A basic microphone circuit was made using a capacitor, resistor, the paper microphone, a signal wire to connect to a speaker, and a ground wire. The setup consisted of fastening the samples to a rigid cardboard frame. Once attached, the samples were tapped and spoken into to test their effectiveness.

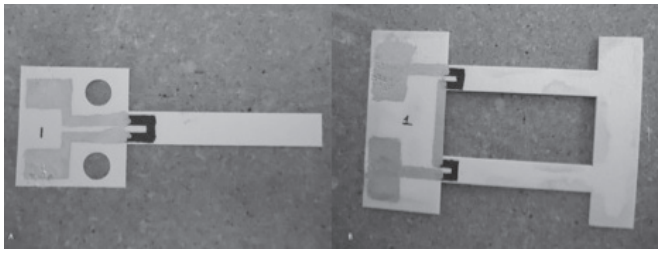

Figure 1: Single and double arm cantilever design.

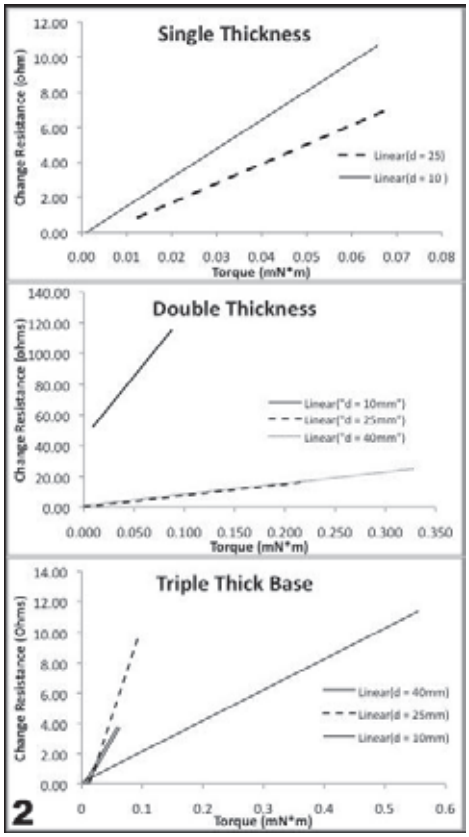

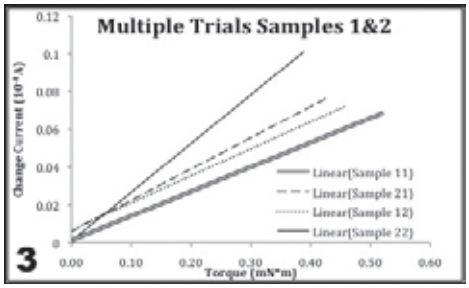

Figure 2, top: Graphs of torque vs. resistance for single arm cantilever for different thicknesses of the cantilever.

Figure 3, bottom: Double arm cantilever trials testing two samples' change of current vs. torque.

Results and Conclusions:

The results from tests done on the single cantilever system showed a linear relationship between force and resistance within our testing range. We found that making contact with the cantilever closer to the base gave the most linear reading, greatest range, and highest resolution. It was found that increasing the base stiffness increased the resolution and gave a more linear reading, but not by a significant amount. When we doubled the thickness of the entire MEMS, there was significant improvement in force range, and linear readings were observed at all tested distances (Figure 2). Upon testing the double arm cantilever, we found that a double thickness design of this model also provided the greatest range and sensitivity. This model was using force as a function of both current and resistance, and linear results were found for both. Figure 3 shows the results for the change of current vs. force test.

We were able to design and construct a paper piezoresistive microphone. Many designs were tested in order to optimize the device and produce the desired results. At first, only taps could be faintly heard through a speaker. We optimized our design even further and then connected to an amplifier. We were then able to clearly distinguish words, proving that the principle works. Upon further design modifications, the microphone was able to transmit music clearly (Figure 4). Further areas of research on this idea would be to condense the sound, diminish background noise, and decrease the size.

Acknowledgements:

I would like to thank Dr. Gary L. Harris and Dr. William L Rose, as well as the rest of the research group at Howard University. I am also thankful to the National Nanotechnology Infrastructure Network Research Experience for Undergraduates (NNIN REU) Program, and the National Science Foundation.

References:

[1] www.memsnet.org

[2] Xinyu, L., et al., "Paper-based Piezoresistive MEMS sensors"; Lab/Chip, 2011, p2189-2196.

[3] www.sensorland.com

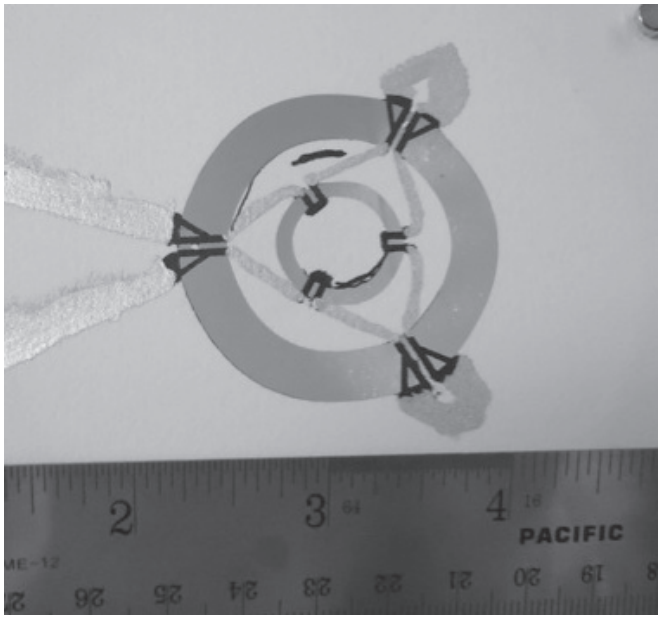

Figure 4: Final working model of the paper microphone.

Fabrication and Characterization of a Micromachined In-Plane Directional Piezoelectronic Microphone

Jia Gloria Lee

Physics, University of California Berkeley

NNIN REU Site: Microelectronics Research Center, The University of Texas at Austin, Austin, TX
NNIN REU Principal Investigator: Dr. Neal A. Hall, Electrical and Computer Engineering, University of Texas at Austin
NNIN REU Mentor: Michael Kuntzman, Electrical and Computer Engineering, University of Texas at Austin
Contact: gloria_lee@berkeley.edu, nahall@mail.utexas.edu, mlkuntzman@gmail.com

Abstract:

The fabrication of a microelectromechanical system (MEMS) microphone, which consists of a beam that responds to a pressure gradient across its longer axis and employs piezoelectronic readout, is described. The advantages of this design included its small form factor, directionality, potentially low self-noise, and the ability to apply active feedback to the system for feedback-altered dynamics. The beam was 2.5 mm × 1.54 mm × 20 μm and fabricated out of silicon (Si). The piezoelectric material used was lead zirconate titanate (PZT). The device's directional response is presented, along with modifications for optimizing the fabrication process.

Introduction:

The purpose of this project was to develop and demonstrate a fabrication process for an in-plane directional microphone that would improve noise performance and source localization in hearing aid and advanced cell phone applications [1]. The microphone was based on a previous design inspired by the parasitoid fly *Ormia ochracea* [2], but replaced the complex optical readout with more elegant piezoelectric readout and modified the pivot mechanism to increase the sensitivity of the microphone.

The microphone consisted of a beam suspended from compliant springs. The beam exhibited high bending stiffness and low rotational stiffness, allowing it to respond to sound traveling along its longer axis (x-axis) by rotating about its shorter axis (y-axis), while preventing it from responding to sound coming in from the top (z-axis) or y-axis by bending. The rocking motion deformed the springs and strained the piezoelectronic material deposited on them, producing a voltage which could be read out (see Figure 1).

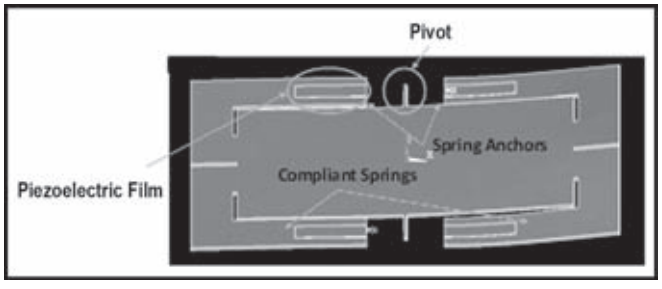

Figure 1: Operational schematic of in-plane directional microphone.

Experimental Procedure:

The device was fabricated on a silicon-with-imbedded-oxide-layer (SOI) wafer. One micrometer (μm) of low-temperature silicon oxide (SiO_x) was deposited on the top as an adhesion layer and 4 μm on the bottom as an etch mask. Titanium (Ti) was evaporated on top using electron-beam evaporation and oxidized in a 700°C furnace to form a 180 nm titanium oxide (TiO_2) diffusion barrier against the PZT.

Top and bottom electrodes for the PZT and electrode bondpads were created by using photolithography to mask the wafer, sputtering 40 nm of Ti for adhesion and 160 nm of platinum (Pt), then lifting off the excess. An 800 nm layer of commercially prepared PZT were deposited using the sol-gel method, patterned with photoresist, and wet-etched in a 200:20:2 mL solution of deionized water : hydrochloric acid : hydrofluoric acid (H_2O:HCl:HF).

The beams and springs were formed by patterning with photoresist and dry-etching through the TiO_2, SiO_x, and epitaxial Si of the SOI wafer with sulfur hexafluoride (SF_6), fluoroform (CHF_3), and SF_6 plasmas respectively. The hinges were formed by depositing 1 μm of sacrificial oxide via plasma-enhanced chemical vapor deposition (PECVD), patterning with photoresist, and dry-etching with CHF_3, then depositing 2 μm of amorphous silicon (a-Si) via PECVD, patterning with photoresist, and dry-etching with SF_6.

A deep silicon etch (DSE) was performed on the backside of the SOI wafer to remove the Si handle layer underneath the beam and springs. A cross-section of the finished device is shown in Figure 2.

Results and Future Work:

Figure 3 shows a scanning electron microscope (SEM) image of the finished device. Some problems with the fabrication process for the top electrode bondpads and hinges were discovered.

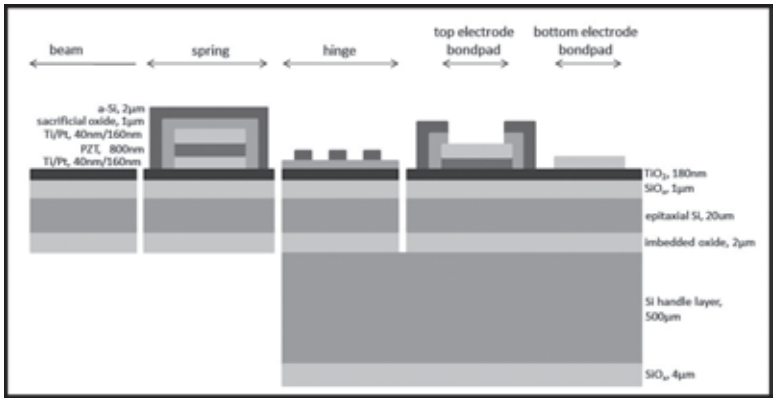

Figure 2: Cross-sectional diagram of finished device.

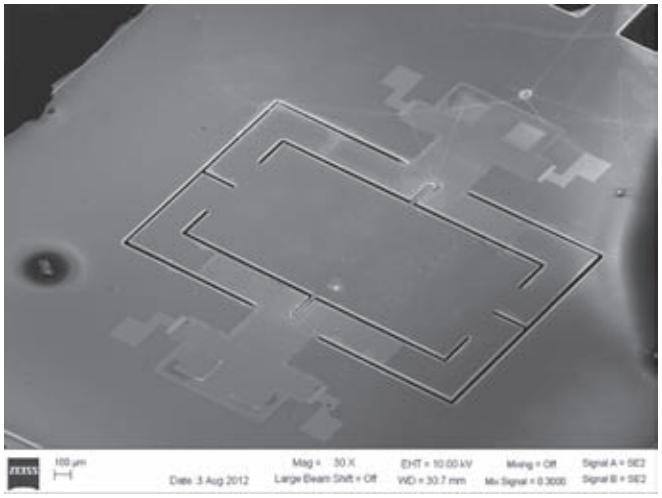

Figure 3: SEM image of finished device.

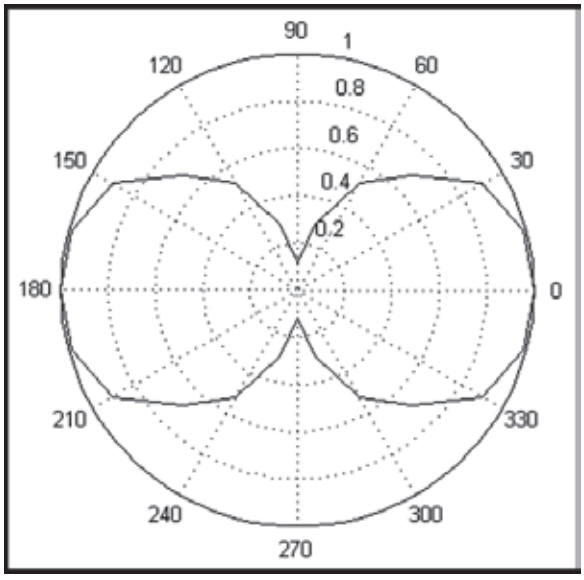

Figure 4: Directivity measurement showing the normalized sensitivity versus angle of incident sound.

The a-Si adhered poorly to the top bondpads and peeled off, especially around the corners. In the subsequent plasma etches, the bondpads were etched through. We attribute the missing top electrode bondpads to two factors: 1) stress from depositing two different materials on top of each other, which caused the silicon to peel off most of the bondpads, leaving them exposed during the SF_6 etch, and 2) insufficient selectivity between the silicon/oxide layers and platinum during dry-etching.

To improve adhesion, we propose depositing a thinner, lower-stress Si layer and/or using circular bondpads instead of square ones to prevent the peeling that occurred around the corners, where the stress was highest. Additionally, depositing a thick layer of chrome over the platinum should reduce selectivity requirements and prevent etching through the bondpads.

The hinges designed to allow the beam to rotate freely did not turn out because the deposited a-Si had bad step coverage. This created discontinuous hinges that would not hold the pins in place if the oxide was etched from underneath. In the future, a silicon deposition method with better step coverage, such as low pressure chemical vapor deposition (LPCVD) poly-silicon, should be used to form the hinge.

In skipping the hinge release step, the hinge became a torsional pivot, allowing the beam to twist about its shorter axis, but preventing it from rotating freely.

Acoustic measurements were performed to determine the directivity of a microphone with a torsional pivot. The microphone was isolated with its x-axis facing a speaker placed 2.5′ away (0° position). The microphone was rotated in 15° increments from 0° to 90° and its sensitivity to acoustic actuation was recorded. The directivity at 11.9 kHz is displayed in Figure 4. The microphone exhibited maximum sensitivity of 14.8 mV/Pa at 0°, and minimum sensitivity of 1.70 mV/Pa at 90°, showing the expected bidirectional polar pattern with 18.8dB difference in sensitivity between the 0° and 90° positions.

Acknowledgements:

I would like to thank my mentor Michael Kuntzman, professor Dr. Neal Hall, the Hall research group, Dr. Marylene Palard, Jeannie Toll, Christine Wood, and the rest of the Microelectronics Research Center staff at UT Austin for their support, guidance, patience, and infinite kindness. I would also like to thank the NNIN REU Program, National Science Foundation, Melanie-Claire Mallison, and Lynn Rathbun for providing this research opportunity.

References:

[1] Amlani, A; "Speech-Clarity Judgments of Hearing-Aid-Processed Speech in Noise: Differing Polar Patterns and Acoustic Environments"; International Journal of Audiology, 45, 319-330 (2006).

[2] Miles, R; "A Low Noise Differential Microphone Inspired by the Ears of the Parasitoid Fly *Ormia Orchracea*"; Journal of the Acoustical Society of America,125, 2013-2026 (2009).